



# Plasma Transferred Arc Deposition of Beryllium

***K. Hollis and B. Bartram***

*Los Alamos National Laboratory, Los Alamos, NM, USA*

**R. Strom, J. Withers**

*MER Corporation, Tucson, AZ, USA*

**J. Massarello**

*Air Force Research Laboratory, Kirtland AFB, NM, USA*

## Abstract

The exceptional properties of beryllium (Be) including low density and high elastic modulus, make it the materials of choice in many defense and aerospace applications. However, health hazards associated with Be material handling limit the applications that are suited for beryllium use. Innovative solutions that enable continued use of Be in critical applications while addressing worker health concerns are highly desirable. Plasma Transferred Arc solid freeform fabrication is being evaluated as a Be fabrication technique for civilian and military space based components. Initial experiments producing beryllium deposits are reported here. Deposit shape, microstructure and mechanical properties are reported.

## Introduction

### Property Requirements

Space based systems for civilian and military applications require extremely lightweight and stiff materials that can survive the harsh conditions of launch and space environmental exposures. In addition, material and fabrication costs must fall within budget for the implementation to be feasible. The primary requirements for space based structural components are:

1. Weight – The components must be ultra lightweight in order to reduce one of the primary cost associated with the mission - launch.
2. Deformation resistance – In order to preserve the required component properties throughout all phases of handling, testing, launch and deployment very high deformation to resistance is required.
3. Fabrication dimensional accuracy – The as-fabricated dimensional accuracy must fall within requirements determined by the mission.
4. Cost – the cost of materials, fabrication and testing must be compatible with the funding allocations for specific missions.
5. Health risk – the risk to workers fabricating, assembling, and testing components must be as low as possible.

### Material Comparison

For a constant weight cylinder, the deformation due to an imposed load varies according to the density cubed divided by the elastic modulus. The figure of merit used for deformation resistance is therefore the elastic modulus divided by the density cubed ( $E/\rho^3$ ) [1]. The advantage of using beryllium over other proposed materials is evident when considering the figure of merit for deformation as shown in Fig. 1. Since the density of Be is low ( $1848 \text{ kg/m}^3$ ) and the elastic modulus is high (303 GPa), the  $E/\rho^3$  value for beryllium is the largest known for any structural material.

### Proposed Technology

In order to produce components at lowest cost with minimal worker exposure to fine particulate Be, near net shape technologies are attractive. Direct casting however, has severe limitations. Beryllium has a high

latent heat of fusion, a relatively high melting point and low thermal conductivity. These factors combine to cause the formation of large columnar grains in cast product. This grain structure limits the mechanical properties of cast Be to ultimate tensile stress values of 34 to 68 MPa and nil ductility [2]. In order to control grain size and improve mechanical properties, Be is typically processed by making powder, consolidating it by vacuum hot pressing, and machining parts from the hot pressed log. However, large, thin walled structures made in this way produce large amounts of material waste. This increases cost, and since the machine chips are a hazardous form of Be particulate, health exposure to workers increases also. The ideal solution is a near net shape fabrication technique which minimizes cost and health risk while also delivering the superior mechanical properties of powder processed Be. Plasma transferred arc (PTA) solid freeform fabrication (SFF) is a technique that injects powder into a focused weld pool to build up structures by adding successive layers to a deposit [3]. By performing PTA SFF of Be in a chamber, the operator is isolated from the Be particulate. Therefore, PTA SFF of Be offers the potential for near net shape fabrication of Be components with low health risks. However, the properties of PTA Be must be evaluated to assess their suitability for space based applications. The investigation described here is the first step in this evaluation process.

## **Experiment**

### Deposition Conditions

Beryllium was deposited by PTA deposition. The PTA torch used was a Eutectic model 220 (Castolin Eutectic Group, Kriftel, Germany) used with an extended anode/nozzle. Argon (99.999% minimum purity) was used as the arc gas, shield gas and powder carrier gas. The arc gas flow rate was 2 standard liters per minute (slm), shield gas flow was 7 slm, and powder gas flow was 2 slm. The torch current was 45 A. Alternating current (AC) at 60 Hz was used for both cathodic arc cleaning on the substrate/deposit and efficient melting of the deposit while minimizing heating of the torch tungsten electrode. The torch was oscillated 10 mm back and forth across the deposit area. The beryllium was deposited on a 304 stainless steel tube with outside diameter 50.8 mm and wall thickness 2.9 mm. The tube was mounted in a rotating fixture and turned at speeds between 0.2 and 2 RPM. Deposition took place in a vacuum chamber that was pumped down and backfilled to atmospheric pressure before deposition. Oxygen levels were maintained below 5 ppm for all deposited material as indicated on an Alpha Omega Instruments Series 3000 trace oxygen analyzer (Alpha Omega Instruments, Cumberland, RI).

### Powder

Gas atomized spherical O-30 Be powder (Brush Wellman, Inc., Cleveland, OH) was used. This powder is shown in the SEM image in Fig. 2 and the particle size distribution is shown in Fig. 3. The chemical composition of the powder is given in Table 1.

Table 1. Beryllium powder chemical composition.

Be	BeO	C	Fe	Al	Si
Bal.	0.64 wt%	0.086 wt%	1090 ppm	425 ppm	325 ppm

### Characterization

The deposited material was characterized by caliper measurements to determine the height and diameter of individual droplets. Deposits were also cut, ground and polished for optical microscopy. Two tensile test samples were machined and pulled to determine mechanical properties. The tensile test samples were 1.47 mm gage diameter with a gage length of 8.8 mm. The samples were pulled at a crosshead velocity of 0.002 mm/s which gives a strain rate of  $2.3 \times 10^{-4}$ /s.

## **Results and Discussion**

### Wetting Behavior

Deposits of Be on stainless steel were found to exhibit poor wetting. Torch/substrate relative motion speed was varied to produce a range of deposit thicknesses. Instead of a smooth bead of material which is possible with good wetting behavior (contact angle of greater than 90°) the Be deposit formed small

solidified droplets as seen in Fig. 4. As the thickness of the deposit was increased, the size of the droplets also increased but still exhibited poor wetting as seen in Fig. 5. The dependence of droplet height on droplet diameter is shown in Fig. 6. There is clearly a scaling effect that maintains a similar ratio of droplet height to diameter. This indicates that the contact angle for the droplets of differing sizes is similar. To determine the contact angle equations 1 and 2 were used

$$H = r + r \cos \theta \quad (1)$$

$$\theta = \arccos (H/r - 1) \quad (2)$$

where H is the droplet height, r is the droplet radius, and  $\theta$  is the contact angle as shown in Fig. 7. Using measured values of H and r (half of the measured width), the contact angle of the droplets has been calculated and is shown in Fig. 8 as a function of droplet height. Figure 8 demonstrates that the contact angle of the droplets ranges from 27° to 67° with an average of 49°. From the data in Fig. 8 the wetting angle does not appear to be a strong function of droplet height and all droplets exhibit poor wetting with contact angles less than 90°.

Young's law relates the contact angle to the surface energies in droplet wetting and is shown in equation 3

$$\Gamma_{s,g} = \Gamma_{s,l} + \Gamma_{l,g} \cos \theta \quad (3)$$

where  $\Gamma_{s,g}$  is the solid/gas surface energy,  $\Gamma_{s,l}$  is the solid/liquid surface energy,  $\Gamma_{l,g}$  is the liquid/gas surface energy, and  $\theta$  is the contact angle shown in Fig. 7. For the Be droplets with  $\theta$  of 49°, the value of  $(\Gamma_{s,g} - \Gamma_{s,l}) / \Gamma_{l,g}$  is 0.66. If this value can be decreased, the wetting angle will increase allowing better wetting and a more controlled Be PTA deposit.

Various surface treatments were used in an attempt to improve the beryllium wetting. The stainless steel was detergent cleaned, sanded clean, cathode arc cleaned, and coated with a TiH flux material. Depositing beryllium on these various surfaces showed little difference in wetting behavior. Pre-heating the substrate to 600°C was also performed to assess the effect on wetting but again little difference was observed. Finally, a 6061 Al alloy tube was used instead of the stainless steel. The various cleaning preparations were also used on the Al tube with no noticeable Be wetting improvement.

#### Continuous Deposit

Because of the poor wetting behavior of Be on stainless steel, thin continuous deposits could not be produced. It was possible to produce a continuous deposit that was 10 mm wide and 5 to 6 mm high. A section of such a deposit is shown in Fig. 9. Typical PTA deposits are in the height range of 1 to 5 mm so the Be deposit is higher than normal. In addition, the deposit to substrate bond was not of high integrity. Since the torch was designed to operate in DC electrode negative mode but was operated in AC mode, the tungsten electrode had a higher heat load than it was designed for. This caused melting and damage to the tungsten when operating above 35 A AC. Changing the tungsten electrode was required to regain easy arc starting after operation above 35A AC. The torch was operated at up to 55 A for short periods of time but was usually kept at 45A to minimize tungsten electrode damage. With this current limitation and the very thick deposit required for bead continuity, there was insufficient current to melt and mix the deposit with the substrate.

#### Be Microstructure

The continuous Be deposit was sectioned and polished to reveal the microstructure. A full height cross section of this deposit is shown in Fig. 10 where the stainless steel substrate is at the bottom of the image. There is a large area of non-contact with the substrate shown in the center bottom of Fig. 10 that appears to be gas porosity. Also, areas of fine porosity are visible at the bottom of the deposit but lessen in volume at the top of the deposit. Figure 11 shows a portion of what is seen in Fig. 10 but at higher magnification. The porosity is observed to be both intra-granular and inter-granular in location. The porosity may be due to dissolved gases (such as N) or low boiling point impurities (such as Mg at 1090°C, Li at 1342°C, Ca at 1484°C, S at 445°C, K at 759°C, or Na at 883°C) in the feed material, which, upon heating, release gas that forms the pores. The grain structure is more clearly resolved in Fig. 11 showing grains ranging from 50 to

750  $\mu\text{m}$  in diameter with an average of around 250  $\mu\text{m}$ . Grain shapes also vary in Fig. 11 with the grains at the top of the image showing equiaxed shapes while the grains near the bottom of the image showing elongated structures in the direction perpendicular to the substrate surface. Since the substrate temperature is cooler than the molten Be, heat is conducted out of the deposit in the direction of the substrate. This heat conduction direction coincides with the long dimension of the columnar grains near the substrate showing the effect of heat conduction on solidification. Farther away from the substrate, the heat flow is more evenly divided between traveling to the substrate and being transferred across the Be free surface to the environment by means of conduction, convection and radiation. This multidirectional heat flow results in more equiaxed grains. Since the Be cooling rate decreases as the distance from the substrate increases, larger grains are seen in the center of the deposit with the largest grains at the top free surface of the Be deposit as is seen in Fig. 10.

### Tensile Test Results

Two small tensile test samples were machined from the continuous Be deposit. One of the samples is shown in Fig. 12. The stress/strain plot from testing is shown in Fig. 13. The 0.2% offset yield stress (YS) for the two samples was 189 and 175 MPa and the ultimate tensile stress (UTS) for the two were 229 and 191 MPa. The strain at failure was 1.4% for the first sample and 0.6% for the second sample. For comparison, stress/strain test results for a commercial hot pressed Be material S200F (Brush Wellman, Cleveland, OH) with the same sample size and test conditions are also shown in Fig. 13. The YS for the hot pressed Be is 221 MPa, the UTS is 377 MPa and the strain at failure is 4.4%. The hot pressed material has a grain size which averages around 12  $\mu\text{m}$ .

Compared to hot pressed Be, the PTA material has lower strength and lower failure strain. This is likely due in part to the porosity in the material as is observed in Figs. 10 and 11. Another large difference between the hot pressed and PTA materials is the grain size. The relationship between grain size and yield stress for steels was formulated by Hall [4] and Petch [5] and is known as the “Hall-Petch equation”. For many materials, including beryllium, the Hall-Petch equation shows that the yield stress of a material is proportional to the inverse square root of the grain size. This is shown in equation 4

$$\sigma_{Y1}/\sigma_{Y2} = d_2^{1/2}/d_1^{1/2} \quad (4)$$

where  $\sigma_{Y1}$  is the yield stress of sample 1,  $\sigma_{Y2}$  is the yield stress of sample 2,  $d_1$  is the grain size of sample 1 and  $d_2$  is the grain size of sample 2. Using the grain sizes of 12 mm for the hot pressed S200F and 250  $\mu\text{m}$  for the PTA Be, equation 4 predicts the yield stress of the hot pressed material to be over four times larger than the yield stress of the PTA material. The actual yield stress of the hot pressed S200F is 1.2 and 1.3 times that of the two PTA samples tested. Viewed in terms of equivalent grain size, the PTA material yield strength is higher than expected compared to hot pressed material.

### Future Research

In order to improve the quality of PTA Be, several changes are required. Beryllium is much more difficult to deposit than most metals due to its poor wetting. This causes individual droplets to form instead of a smooth thin continuous deposit. In order to form a continuous deposit, the Be thickness must be greater than about 5 mm. This thick deposit causes slower cooling rates in the material and increases subsequent grain growth. If a substrate/atmosphere combination can be found which increases wetting of the Be molten pool, a thinner deposit could be realized. This thinner deposit would most likely have smaller grain size and would allow for better dimensional control of the deposit. The smaller grain size would improve mechanical properties and the better dimensional control would allow fabrication of near net shape parts with less finish machining required to achieve final shape. Better thermal contact between the deposit and the substrate will also result in faster cooling rates and smaller grain sizes. A PTA torch capable of 100 A AC output would give better substrate heating and improve the deposit bond quality. Decreasing the porosity of the deposit is also required to optimize properties. This may be improved by more careful control of impurities in the powder feed material and/or the environment surrounding the molten Be during deposition. In addition, a wider variety of deposition conditions could be investigated in hopes of suppressing pore formation or allowing the gas phase material to migrate to the free surface of the Be due to buoyancy forces and be released.

## Conclusions

The following conclusions resulted from this investigation:

- PTA deposited Be exhibits poor wetting on stainless steel and aluminum giving solidified particle wetting contact angles between 27° and 67°.
- Depositing a thick (more than 5 mm) single pass of width 10 mm allows for a continuous deposit of PTA Be to be formed.
- The PTA Be deposit has both intra-granular and inter-granular porosity which is most pronounced near the deposit/substrate interface and decreases in volume near the Be free surface.
- The PTA Be deposit has widely ranging grain size in the range of 50 to 750 µm.
- The tensile yield stress (0.2% strain offset) of the PTA Be samples was 189 and 175 MPa and the ultimate tensile stresses were 229 and 191 MPa.
- The strain at fracture for the PTA Be samples was 1.4% and 0.6%.
- The mechanical properties of the initial PTA Be samples are inferior to commercial hot pressed S200F Be.
- After accounting for grain size effects in the material, the PTA Be yield stress compares favorably to that of hot pressed commercial Be.
- If future research can bring improvements to the molten Be wetting and the substrate/deposit interfacial heat transfer and if trapped porosity can be eliminated, decreased grain size and better dimensional control of the deposit are expected. If this can be realized, PTA SFF Be offers potential improvements in cost and worker health risks over traditional powder processed Be.

## Acknowledgement

This work was funded by an STTR grant from the Missile Defense Agency. The assistance of Rick Lauer, Ed Coennen, Sam Attencio, Bill Taylor, and Marty Mataya is gratefully acknowledged for machining, polishing, and mechanical testing work.

## References

1. E. Roussel, J.P. Fromentin, A. Freslon, Realization of Mirror Shells for X-Ray Telescope by Plasma Forming, *Thermal Spray: Meeting the Challenges of the 21<sup>st</sup> Century*, C. Coddet Ed. ASM International, Materials Park, OH, 1998.
2. R.W. Krenzer, Casting, *Beryllium Science and Technology*, Vol. 2, D.R. Floyd and J.N. Lowe, Eds., Plenum Press, 1979, p. 31-56.
3. H. Wang, W. Jiang, M. Valant, R. Kovacevic, Microplasma Powder Deposition as a New Solid Freeform Fabrication Process, *Proc. Instn Mech. Engrs. PartB: J. Engineering Manufacture*, Vol 217, 2003, p. 1641-1650.
4. E.O. Hall, Deformation and Ageing of Mild Steel, *Proc. Phys. Soc.*, Vol 64 (No. 381B) 1951, p.747-753.
5. N.J. Petch, Cleavage Strength of Polycrystals, *J. Iron Steel Inst.*, Vol 174 (Part 1) 1953, p. 25-28.

## Figures

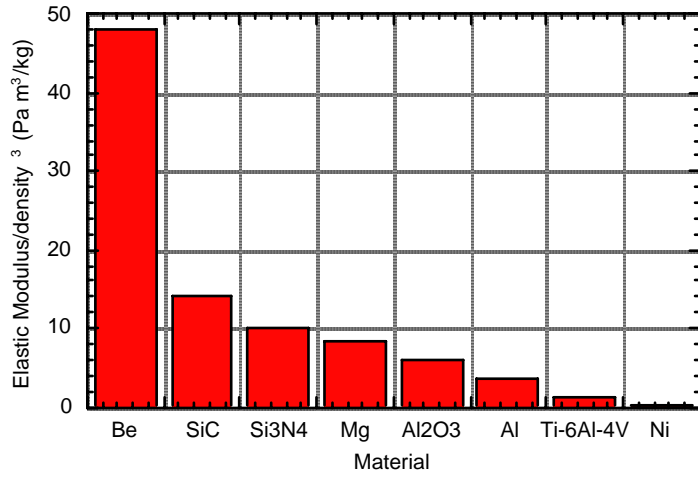


Fig. 1. Material comparison for cylindrical figure of merit for space structures.

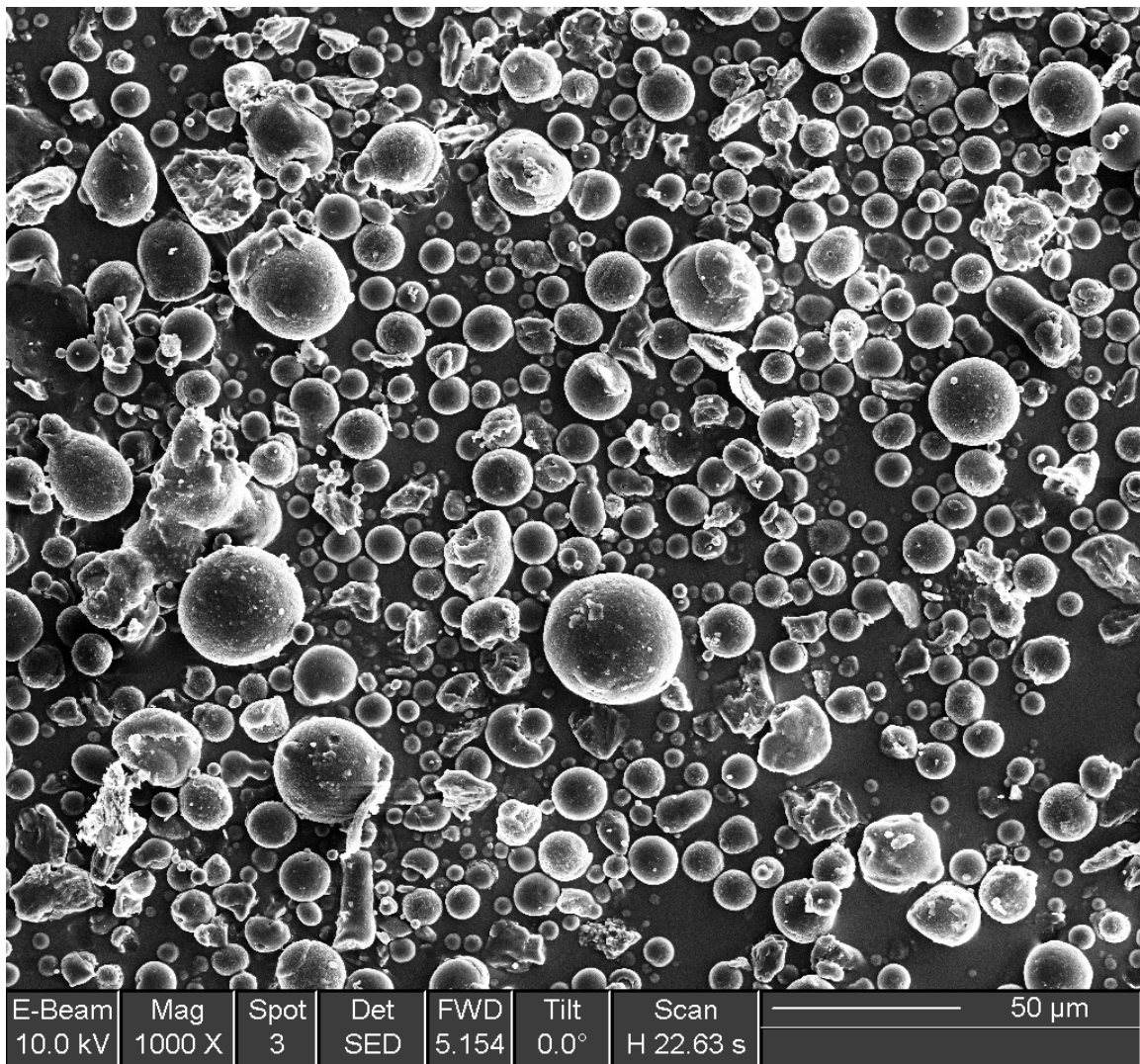


Fig. 2. SEM image of beryllium powder used for PTA deposition.

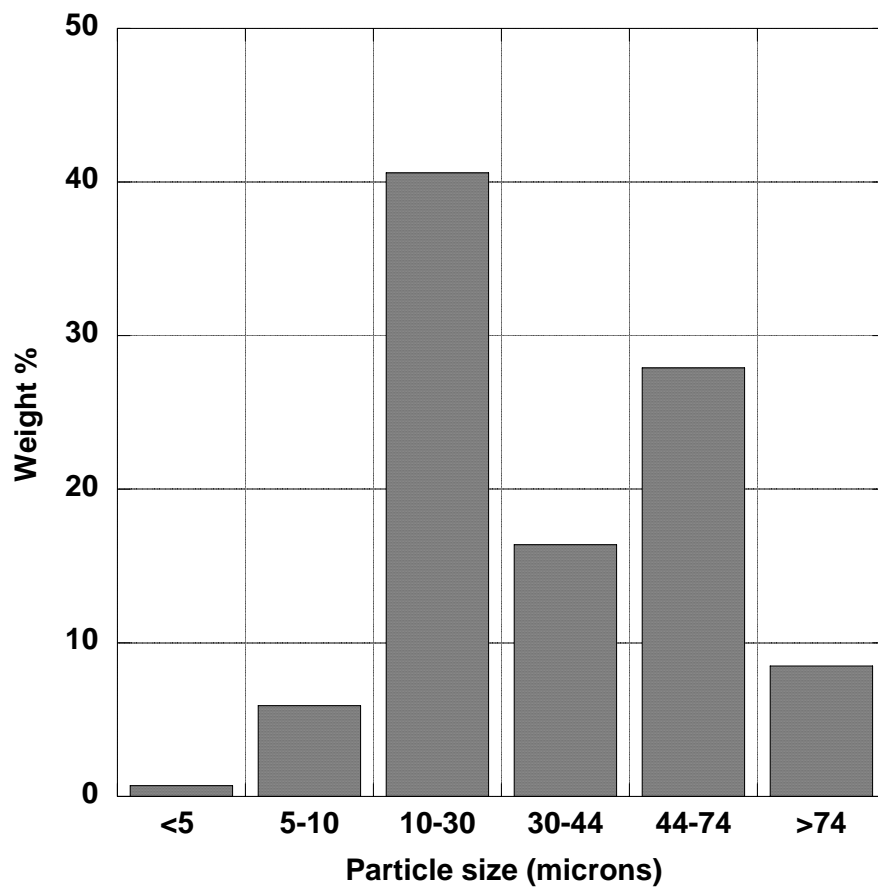


Fig. 3. Beryllium powder size distribution.



Fig. 4. Small beryllium droplets with poor wetting on the stainless steel substrate. For scale reference, the deposit width is 11 mm.



Fig. 5. Beryllium deposit on stainless steel. Deposit width is 11 mm.

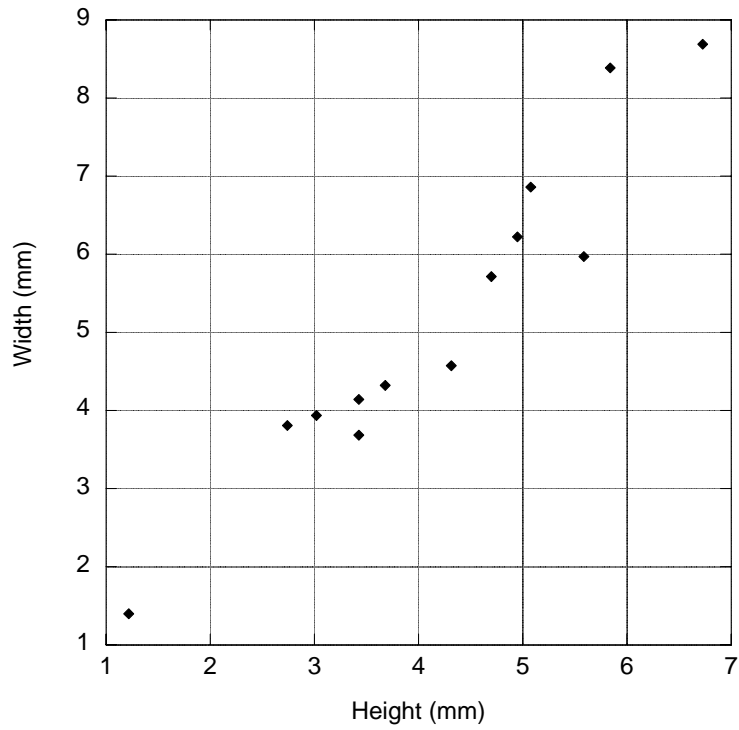


Fig. 6. Beryllium droplet height and width for poor wetting material.

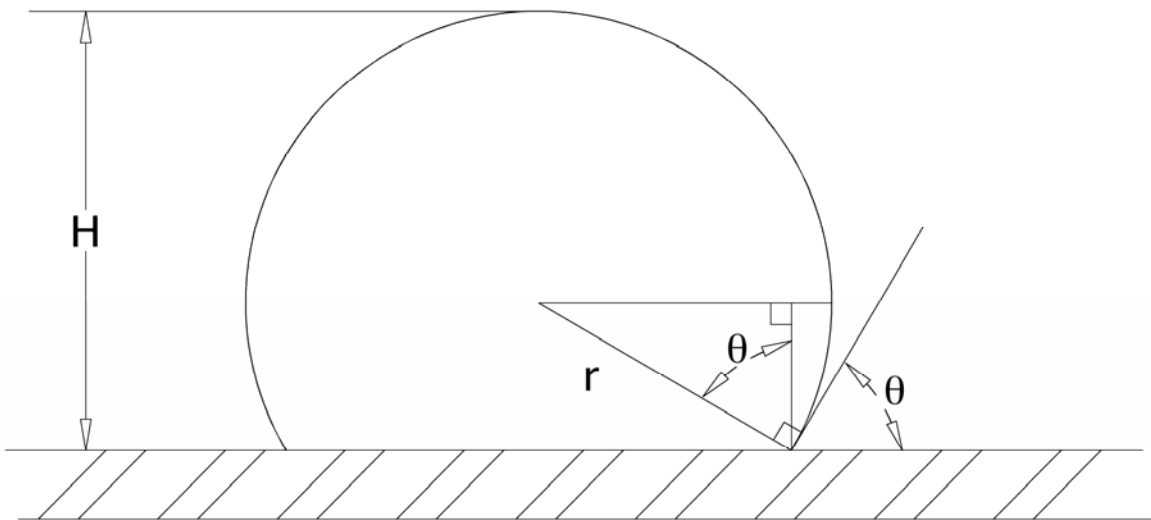


Fig. 7. Drawing of droplet geometry showing droplet height ( $H$ ), radius ( $r$ ) and contact angle ( $\theta$ ).

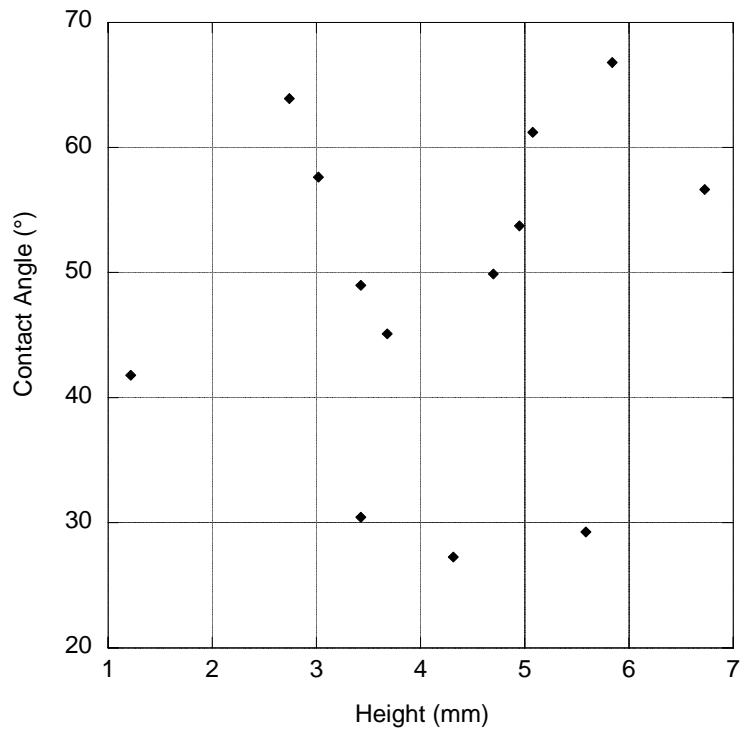


Fig. 8. Wetting angle as a function of droplet height for beryllium deposited on stainless steel.



Fig. 9. Continuous beryllium deposit on stainless steel. Deposit height is 6 mm and width is 10mm.

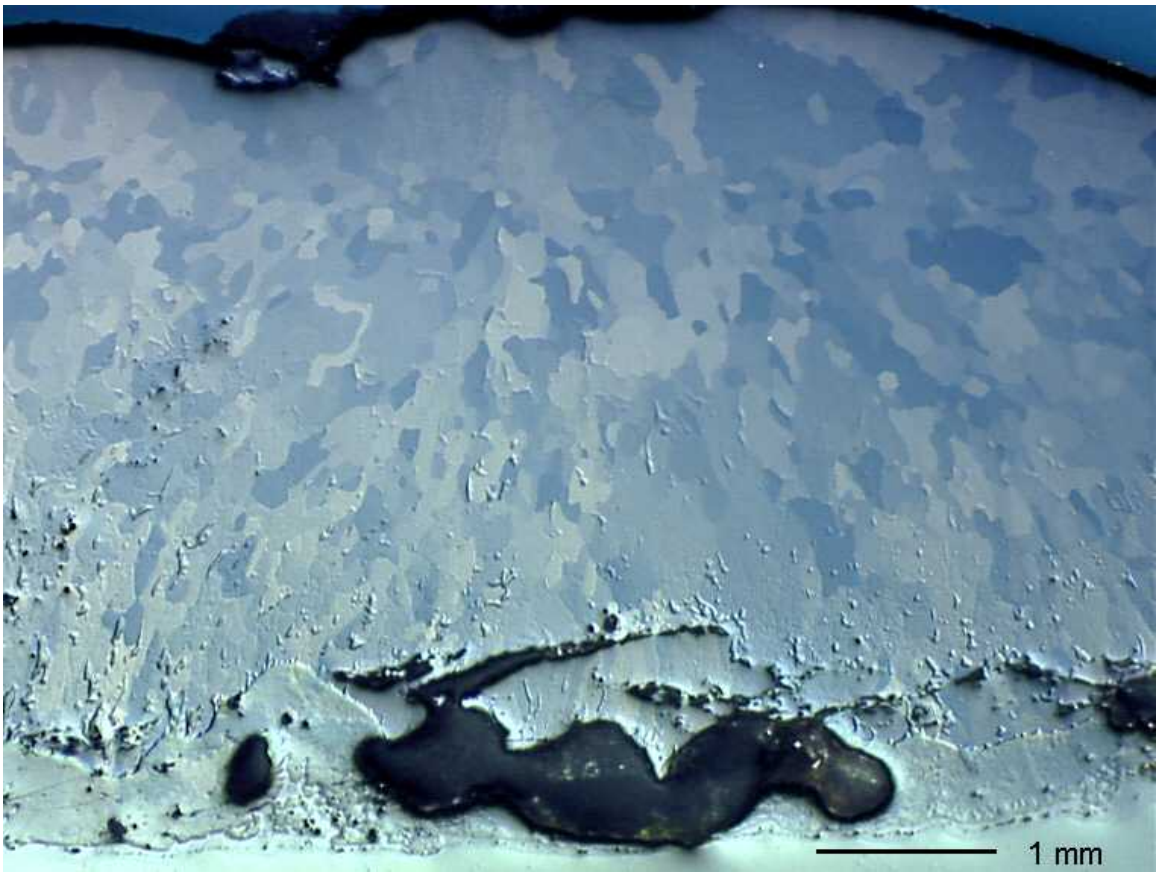


Fig. 10. Full height cross section of Be deposit.

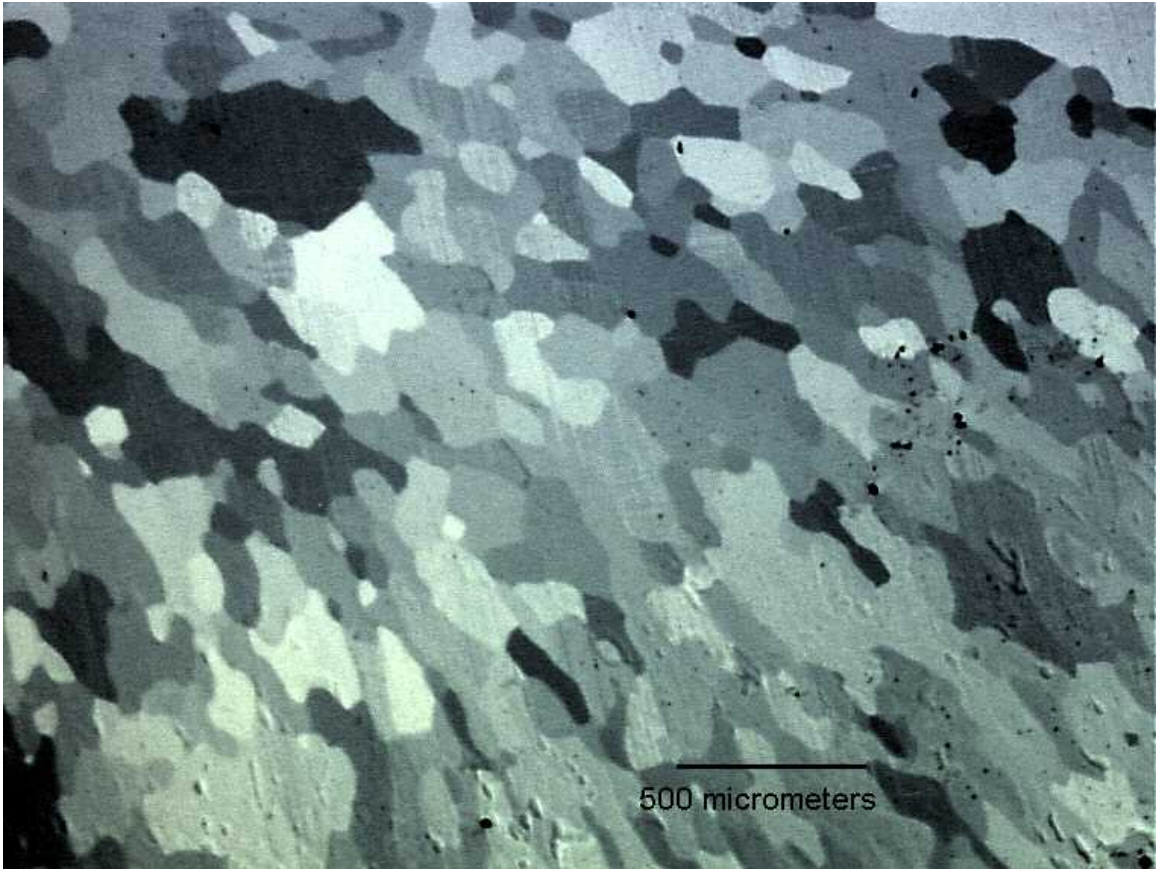


Fig. 11. Cross section of Be deposit.



Fig. 12. Be tensile test sample. The sample is 1.47 mm gage diameter with a gage length of 8.8 mm.

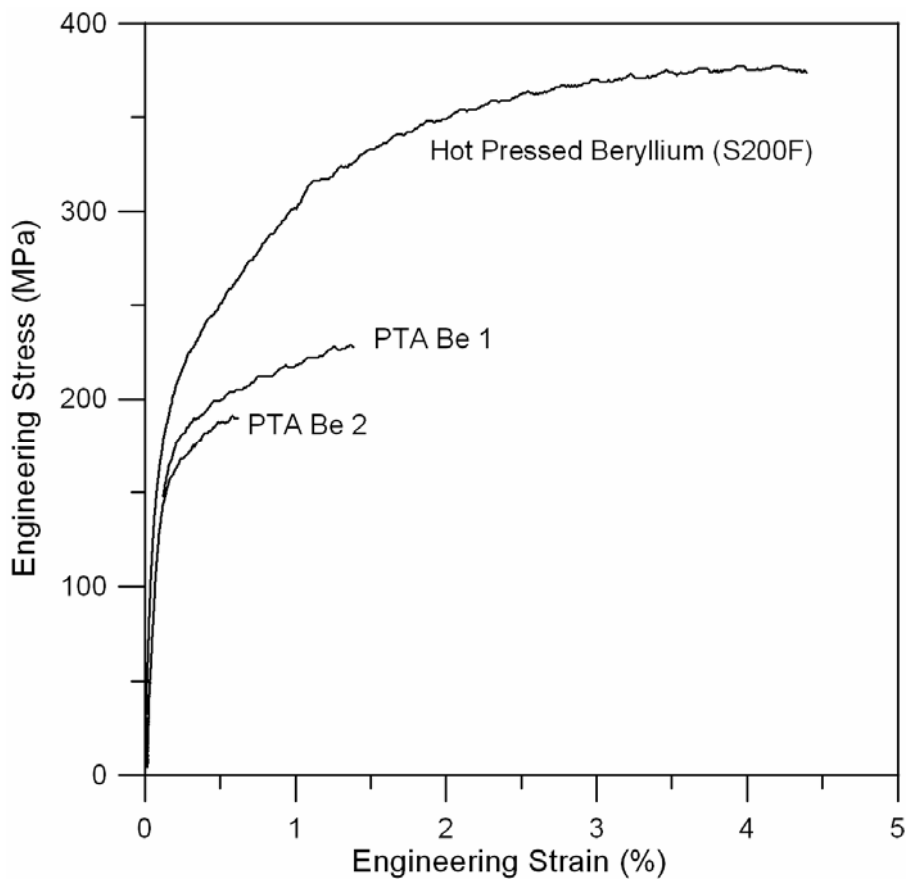


Fig. 13. Tensile stress/strain plot for the two PTA Be samples and one hot pressed commercial sample.